Annals of Hematology & Oncology

Open Access

Austin Publishing Group

Research Article

Olaparib Induced Moderate Killing of *ATM*-Deficient Mantle Cell Lymphoma Cells *In Vitro* and *In Vivo*

Kiel PJ[1,2]*, Overholser BR[3], Feng H[1], Sinn A[1], Riley AA[1], McCarthy PB[1], Pollok K[1], Territo PR[1] and Srivastava S[4]

[1]Indiana University School of Medicine, USA
[2]Indiana University Simon Cancer Center-IU Health, USA
[3]Purdue University College of Pharmacy, USA
[4]Bristol-Myers Squibb-Global Pharmaceutical Company, USA

***Corresponding author:** Patrick J Kiel, Indiana University School of Medicine, USA

Received: December 26, 2018; **Accepted:** February 01, 2019; **Published:** February 08, 2019

Abstract

The Ataxia Telangiectasia Mutated (*ATM*) gene is frequently inactivated in lymphoid malignancies such as and Mantle Cell Lymphoma (MCL) and is associated with defective apoptosis, especially in response to standard cytotoxic chemotherapy. *ATM* deficient cells exhibit impaired homologous recombination and the inability to correct double strand DNA breaks. Inhibition of poly (ADP-ribose) Polymerase (PARP), which is required for DNA double strand break repair, has been shown to sensitize *ATM*-deficient tumor cells to killing. We investigated *in vitro* and *in vivo* sensitivity to the PARP inhibitor olaparib in the *ATM* deficient mantle cell lymphoma cell line Granta-519. Olaparib monotherapy and in combination with cisplatin or bendamustine confirmed decreased proliferation *in vitro*. A Nonobese Diabetic/Severe Combined Immunodeficient (NOD/SCID) murine xenograft model with the Granta-519 cell line did not result in a significantly reduced tumor load following treatment with olaparib *in vivo*.

Keywords: Ataxia telangiectasia; PARP; Mantle cell; Granta-519; Olaparib

Introduction

Cancer is a disease of genomic instability and can arise through aberrant DNA double strand breaks leading to the formation of chromosomal translocations, deletions, and inversions. These genomic aberrations occur at an increased frequency in cells with inherited or somatically acquired mutations that results in compromised DNA repair mechanisms. Hereditary mutations of genes involved in homologous recombination, such as Ataxia Telangiectasia (*ATM*), Breast Cancer (BRCA) [1,2], and TP53 can result in an increased risk of cancer development.

ATM is a serine/threonine protein kinase that initiates cell cycle checkpoint signaling in response to DNA damage secondary to radiation or alkylator based therapy [3-5]. Deficiency of *ATM* exhibits radio sensitivity, loss of cell cycle checkpoints, and p53. Following DNA damage, cells with *ATM* deficiency displays prolonged DNA Double Strand Breaks (DSB) and retention of DNA proteins at the site of these breaks as intra-nuclear foci [4-8]. Similar to BRCA loss of function genes, *ATM* loss or deficiency leads to cancer cells relying on single strand DNA repair mechanisms from Poly (ADP-ribose) polymerase-1 (PARP-1).

Synthetic lethality using PARP inhibitors has emerged as a new potential therapeutic strategy to exploit tumor-specific genetic alterations. Synthetic lethality is defined as the premise, whereby, deletion of one of two genes independently has no effect on cellular viability, whereas, simultaneous loss of both genes is lethal. The utility of this approach was first demonstrated when cells with mutations in the breast and ovarian susceptibility genes *BRCA1* and *BRCA2* were shown to be extremely sensitive to small molecule inhibitors of the DNA Single Strand Break (SSB) sensing protein PARP-1.

Deficiency of *ATM* occurs in 20-50% of Mantle Cell Lymphoma (MCL) cases and has the largest incidence of any non-Hodgkin's subtype [9,10]. MCL is a B-cell non-Hodgkin lymphoma characterized by the genetic hallmark of a chromosomal translocation t(11;14) resulting in aberrant cyclin D1 expression [11]. *In vitro* data evaluating monotherapy of the PARP-inhibitor olaparib in *ATM*-deficient B-cell chronic lymphocytic leukemia induced significant killing through mitotic catastrophe independent of apoptosis [7]. Additionally, in lymphoid cell lines Granta-519 and UPN2, which have low levels of *ATM*, olaparib decreased tumor growth [3]. In this study we investigated the PARP inhibitor olaparib with standard chemotherapy used to treat MCL *ATM* deficient lymphoid tumors.

Methods

Cell proliferation assay

Suspensions of the lymphoid Granta-519 cells which were provided by Drs. Chen and Plunkett at MD Anderson Cancer Center were exposed to increasing concentrations of olaparib (Selleck Chemicals, Houston, TX) and chemotherapy (cisplatin; bendamustine) for up to 72 hours. Tumor growth potential was established using the Cell Titer 96 cytotoxicity assay (Promega, Madison, WI). An amount of 40µl of the tetrazolium dye was added to each well of the plate and then incubated for an additional 4 hours. Optical Density (OD) was read directly at 492nm using the automated Dynex plate reader.

Western Blotting

Protein was loaded and run on Any kD Mini-PROTEAN TGX precast-polyacrylamide gel, transferred to nitrocellulose membranes (Bio-Rad Laboratories®), and blocked. Membranes were developed following exposure to the following antibodies: Annexin V (Santa Cruz Biotechnology Inc.); mouse anti-CHEK1,mouse anti-CHEK2, rabbit anti-cleaved caspase 7, rabbit anti-cleaved caspase 3, and rabbit anti-GAPDH (Cell Signaling Technology, City St); rabbit anti-cleaved PARP(Asp214), rabbit anti-PARP antibody, mouse anti-Phospho-p53(Ser15) and mouse anti-p53 antibody from Cell Signaling Technology; rabbit anti-Bax antibody 50 and rabbit anti-Bax antibody 100 from Biolegend.

Citation: Kiel PJ, Overholser BR, Feng H, Sinn A, Riley AA, McCarthy PB, et al. Olaparib Induced Moderate Killing of *ATM*-Deficient Mantle Cell Lymphoma Cells *In Vitro* and *In Vivo*. Ann Hematol Oncol. 2019; 6(2): 1233.

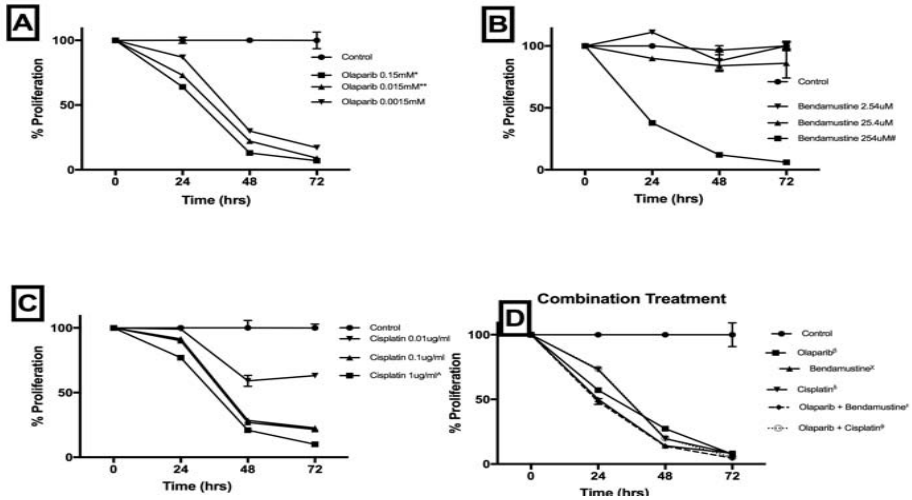

Figure 1: Cytotoxic Results in ATM deficient Granta-519 Mantle cell lines.
Proliferation of Granta519 mantel cell lymphoma cell lines following exposure to bendamustine, cisplatin, and olaparib at increasing cytotoxic concentrations. In combination: bendamstine 254μM plus olaparib 0.15mM, cisplatin 1μg plus olaparib 0.15mM and monotherapy of olaparib 0.15mM, cisplatin 1μg, and bendamustine 254μM. Analyzed with ANOVA and Dunnett's multiple comparisons test: *p=0.0163, **p=0.0272, #p=0.0063, ^p=0.0221, βp= 0.0046, χp=0.0022, εp=0.0064, δp=0.0018, ϕp=0.0059.

Murine xenograft model

The lymphoid cell line Granta-519 was mixed with Matrigel (BD Bioscience) and injected subcutaneously (200μl containing 10×10^6 Granta-519) into the right flanks of 6-8 week-old immunocompromised NOD/SCID mice. Tumor growth was monitored twice weekly by measurement of the long and short diameters of the tumor using calipers. Caliper measurement of the longest perpendicular tumor diameter was performed to estimate the tumor volume, using the following formula: $4\pi/3\times(\text{tumor width}/2)^2\times(\text{tumor length}/2)$, representing the three-dimensional volume of an ellipse. When the tumor volume reached approximately 100-200 mm^3, mice were randomly assigned into treated groups. The maximum volume observed was 2656mm^3. Body weight endpoints were not collected. Treatment groups included: vehicle control (n=6), olaparib starting on day 7 of implant at 50mg/kg/day Monday through Friday, no more than 28 days of treatment (n=6), bendamustine 10mg/kg on day 7 and day 14 (n=6); olaparib 50mg/kg/day Monday through Friday, no more than 28 days of treatment plus bendamustine 10mg/kg on day 7 and 14 (n=6). Drugs and control vehicle were be administered by gavage feeding (olaparib) or intraperitoneal injection (bendamustine). Mice were sacrificed at 8 weeks after drug treatment or when they become moribund (if earlier).

All studies were carried out in accordance with, and approval of, the Institutional Animal Care and Use Committee of Indiana University School of Medicine, and the Guide for the Care and Use of Laboratory Animals (IACUC study #10416). NOD/scid mice were obtained from the *in vivo* Therapeutics Core of the Indiana University Simon Cancer Center. Animals were maintained under pathogen-free conditions and maintained on Teklad Lab Animal Diet (TD 2014, Harlan Laboratories USA) with *ad libitum* access to sterile tap water under a 12-hour light-dark cycle at 22-24˚C. All techniques are established such that experiments are conducted in the most efficient manner and using the minimum number of animals. Mice monitoring occurred daily for determine of weight and general appearance. Mice were euthanized immediately if any of the following are evident: Failure to eat and drink for >48 hours; rapid loss of 15-20% body weight; inactivity with hunched posture; lesions that interfere with ability to eat and drink; evidence of self-mutilation, lesions with major ulcerating surfaces; loss of righting reflex and inability to maintain upright posture; loss of general body condition with spine becoming visible; dehiscence of wounds and/or evidence of infection not responsive to veterinary treatment. Euthanasia occurred with CO_2 inhalation followed by cervical dislocation as a secondary method.

In vivo Bioluminescent Imaging (BLI)

***In vivo* Imaging:** *In vivo* imaging was performed as described by Shannon et al, with some minor modifications [12]. Briefly, post tumor implantation and continuing weekly thereafter, dynamic bioluminescence images were acquired on a Berthold NightOwl (Berthold Inc. USA) at 40˚C, where up to 3 mice per session were simultaneously scanned. In denuded mice, anesthetic induction was achieved with 2-4% isoflurane, and animals were administered 150mg/kg D-luciferin (Caliper Lifescience USA) subcutaneously. Mice were sequentially imaged at 2 min intervals for 40 mins with image integration times ranging from 1 to 120 sec/image. At the completion of the sequence, anatomical reference photos were also acquired to generate fused image sets.

Image analysis: To provide visualization, segmentation and time series quantification from the 40 min scan, BLI and anatomical reference images were imported into custom developed software (*eLumenate*, developed by Dr. Territo). Pseudo-colored parametric overlays of BLI time-series with anatomical reference images were dynamically constructed for each animal. Using the image of the time series with the peak light emission for each individual animal, ROIs were designated for both primary tumors and a metastatic region. Primary tumors were segmented through time using the semi-

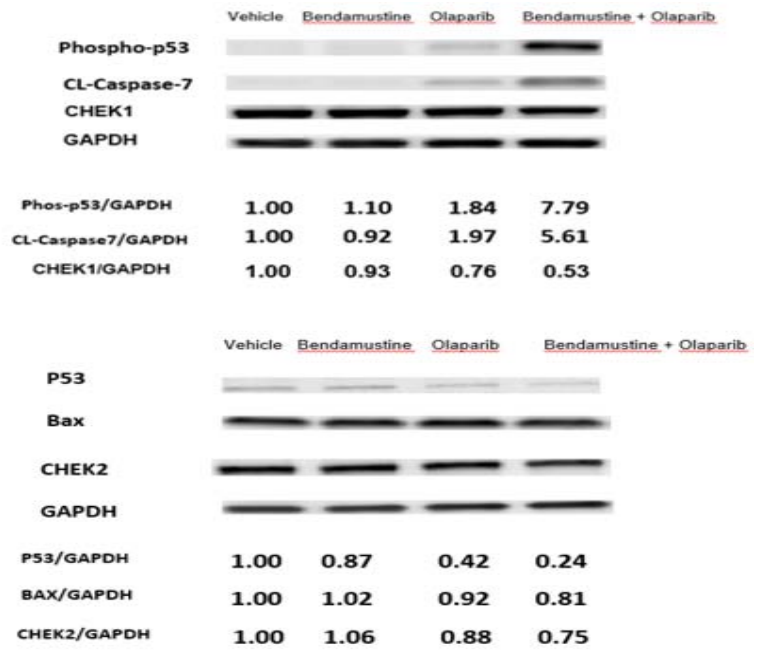

Figure 2: Treatment with olaparib in ATM deficient Granta-519 sensitized to cytotoxic chemotherapy.
Western blot analysis of Granta-519 cells showing increased cleavage of PARP1, caspase 7, cleaved caspase-7, and phospho-53 after olaparib montherapy or in combination with bendamustine. Granta-519 cells treated with bendamustine 127μM and or olaparib 7.5mM for 24 hours.

automated maximum entropy ROI algorithm [13]. The extracted time series were then analyzed for average emission flux density in a region and the integral of emission flux according to:

$$I_A(n,t) = \frac{1}{m}\sum_{i=1}^{m} I_p(i,t) \quad (1)$$

$$AUC(n,x) = \int_a^b I_A(j,n,t)\,dx \quad (2)$$

Where, I_A, I_P, i, n, m, a, b, x, AUC and t are the average emission flux density (Ph/s*mm^2), pixel emission flux density, pixel, subject, total number of pixels, integration start, integration end, integration interval, area under the curve (Ph/mm^2), and time points, respectively. To minimize the role of tumor and animal motion on time course parameters, individual ROIs across image frames were aligned by computing the per frame center of gravity [14] offset between successive frames, and applying the x-y offset to the ROI prior to computing I_p or I_A described in equations 1 or 2, respectively.

Statistical analysis

In vitro Data are presented as means +/- SD and analyzed using ANOVA followed by Dunnett's test of multiple comparison. Statistical difference in tumor volume were determined using the Student's t test. GraphPad Prism 7 software (GraphPad Software, Inc., La Jolla, CA, USA) was used to perform all statistical analysis, using Student's t test or nonparametric Mann-Whitney test/ANOVA for comparisons between groups of samples.

Results

ATM deficient lymphoid tumor cell sensitivity to PARP inhibition and cytotoxic therapy

To assess the ability of PARP inhibition to increase the effect of standard mantle cell lyphoma therapy, we tested the ability of olaparib to sensitize *ATM* mutant Granta-519 cells to cisplatin and bendamustine (Figure 1). The percent proliferation of lymphoid cells was at 24, 48, and 72 hours with olaparib 0.15mM monotherapy was 63.9%, 12.9%, and 6.56%, respectively. However, the addition of olaparib to cisplatin or bendamustine provide a similar rate of efficacy against Granta-519 proliferation.

Apoptosis, caspase, and downstream activity (western blots results)

To assess the effects of olaprib and bendamustine on downstream molecules, we used Western blot analysis (Figure 2) to observed p53, phosphorylated 52, caspase, cleaved PARP, and ANNEXIN. Inhibition of PARP-1 leads to the accumulation of DNA single-strand breaks that are converted to DSBs during DNA replication [1,2,8]. In cells with defects in DSBs, CHEK pathways may be relied upon for single-strand repair. To assess this we evaluated CHEK1 and CHEK2 accumulation. Bax was analyzed as it has been observed to be increased with bendamustine initiated apoptosis [15].

The results indicated that the bendamustine and olaparib combination resulted in an increase in cleaved PARP, cleaved caspase 7, and phopho-53. No difference was observed in CHEK1 or CHEK2.

Effect of olaparib with or without cisplatin or bendamustine in a Granta-519 Xenograph model

To investigate the *in vivo* impact of olaparib, we generated murine xenograft models of the *ATM* deficient cell line, Granta-519 cell at a volume of 100cells/mm^3 injected subcutaneously into the right flanks. Tumors were assessed *via* caliper and bioluminescent imaging (Figure 3). Following inoculation mice were treated with vehicle control, olaparib, bendamustine, or olaparib plus bendamustine.

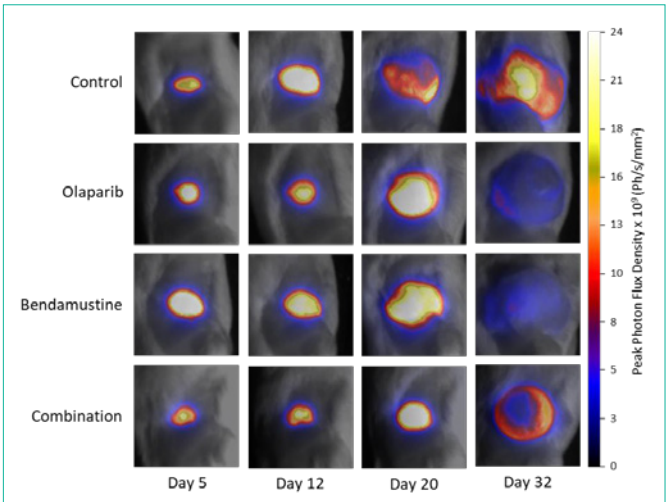

Figure 3: Tumor distribution pattern of one representative animal per treatment during days 5, 12, 20, and 32. In all cases, data are shown as peak emission photon density (Ph/s.mm^2) and are scaled uniformly across subject and time.

One mouse death was likely dosing related while the rest were alive at 34 days post lymphoma implantation. Combination therapy with bendamustine and olaparib produced a modest lag in lymphoma growth. Mean tumor volume on day 34 of caliper measurement was 1732.1cells/mm^3 +/- 1029.2cells/mm^3 for the control *vs.* 1317.6cells/mm^3 +/- 399cells/mm^3 (p=0.421) for the olaparib plus bendamustine combination (Figure 3).

Discussion

ATM deficiency in mantle cell lymphomas pose an interesting target in the era of precision medicine. The synthetic lethality approach is a novel therapeutic intervention, which has been validated clinically in ovarian cancers with regards to BRCA mutations [16]. Evaluation of BRCA mutation in the role of malignancy has led to the approval of olaparib, rucaparib, and niraparib in ovarian cancer, as well as, olaparib in BRCA mutated breast cancer. The Phase III OlympiAD trial in breat cancer showed a reduced risk of disease progression or death by 42% with olaparib compare to physicians choice chemotherapy [21]. Previous *in vitro* data suggested by Weston et al, provides efficacy data with olaparib as monotherapy in *ATM* deficient chronic leukemia cell lines [8].

In this current study, we demonstrated that the PARP inhibitor olaparib is able to enhance a pre-existing DNA repair defect in an *ATM* deficient mantle cell lymphoma cell line, Grant-519. The growth of *ATM* deficient Granta-519 tumor cells in a NOD/SCID xenograph model was not significantly decreased by olaparib monotherapy or combination therapy. Tumor volumes were assess by caliper measurements and *via* bioluminescent quantification. While a more pronounced benefit was observed with caliper measurement, bioluminescent imaging demonstrates the ability to detect microscopic tumors and provide a more accurate assessment of estimated tumor volumes *in vivo* [17]. In this study further evaluation with BLI did not support a significant decrease in Grant-519 growth with olaparib as monotherapy or in combination with bendamustine with regards to the *in vivo* model. Others studies have suggested that *ATM* deficient lymphomas with concomitant p53 and ATR mutations may allow for greater sensitivity to olaparib [18,19]. Evaluating several mutations that may affect the lymphoma's response to treatment is a next logical step in assessing synthetic lethality based therapy and may include a myriad of interdependent pathways such as the following: p53, ATR, CHEK1, CHEK2, loss of heterozygosity and levels of PARP expression [18-21].

Acknowledgement

This publication and project is supported by a research grant from the Hematology/Oncology Pharmacy Association (HOPA). The content is solely the responsibility of the authors and does not necessarily represent the official views of HOPA. This publication and project is supported by Indiana University Health, Indianapolis, IN with assistance from the Indiana Clinical and Translational Sciences Institute, and is funded in part by Grant # UL1TR001108 from the National Institutes of Health, National Center for Advancing Translational Sciences, Clinical and Translational Sciences Award.

The content is solely the responsibility of the authors and does not necessarily represent the official views of the National Institutes of Health.

References

1. Farmer H, McCabe N, Lord CJ, Tutt AN, Johnson DA, Richardson TB, et al. Targeting the DNA repair defect in BRCA mutant cells as a therapeutic strategy. Nature 2005; 434: 917-921.
2. Bryant HE, Schultz N, Thomas HD, Parker KM, Flower D, Lopez E, et al. Specific killing of BRCA2-deficient tumours with inhibitors of poly(ADP-ribose) polymerase. Nature. 2005; 434: 913-917.
3. Williamson CT, Muzik H, Turhan AG, Zamò A, O'Connor MJ, Bebb DG, et al. ATM Deficiency Sensitizes Mantle Cell Lymphoma Cells to Poly(ADP-Ribose) Polymerase-1 Inhibitors. Mol Cancer Ther. 2010; 9: 347-357.
4. Shiloh Y. The ATM-mediated DNA-damage response: taking shape. Trends Biochem Sci. 2006; 31: 402-410.
5. Lavin MF. Ataxia-telangiectasia: from a rare disorder to a paradigm for cell signalling and cancer. Nat Rev Mol Cell Biol. 2008; 9: 759-769.
6. Löbrich M, Jeggo PA. The impact of a negligent G2/M checkpoint on genomic instability and cancer induction. Nat Rev Cancer. 2007; 7: 861-869.
7. Taylor AM, Byrd PJ. Molecular pathology of ataxia telangiectasia. J Clin Pathol. 2005; 58: 1009-1015.
8. Weston VJ, Oldreive CE, Skowronska A, Oscier DG, Pratt G, Dyer MJ, et al. The PARP inhibitor olaparib induces significant killing of ATM-deficient lymphoid tumor cells *in vitro* and *in vivo*. Blood. 2010; 116: 4578-4587.
9. Schaffner C, Idler I, Stilgenbauer S, et al. Mantle cell lymphoma is characterized by inactivation of the ATM gene. Proc Natl Acad Sci. USA. 2000; 97: 2773-2778.
10. Fang NY, Greiner TC, Weisenburger DD, Chan WC, Vose JM, Smith LM, et al. Oligonucleotide mirco-arrys demonstrate the highest frequency of ATM mutations in the mantle cell lymphoma subtype of lymphoma. Proc Natl Acad Sci USA. 2003; 100: 5372-5377.
11. Perez-Galan P, Dreyling M, Wiestner A. Mantle cell lymphoma: biology, pathogenesis, and the molecular basis of treatment in the genomic era. Blood. 2011; 117: 26-38.
12. Shannon HE, Fishel ML, Xie J, Gu D, McCarthy BP, Riley AA, et al. Longitudinal Bioluminescence Imaging of Primary *versus* Abdominal Metastatic Tumor Growth in Orthotopic Pancreatic Tumor Models in NSG Mice. Pancreas. 2015; 44: 64-75.
13. Sin CF, Leung CK. Image segmentation by edge pixel classification with maximum entropy. IEEE Xplorer; Proceedings of the International Symposium on Intelligent Multimedia, Video and Speech Processing. 2001; 283-286.

14. van Assen HC, Egmont-Petersen M, Reiber JH. Accurate object localization in gray level images using the center of gravity measure: accuracy *versus* precision. IEEE Trans Image Process. 2002; 11: 1379-1384.

15. Schwanen C, Hecker T, Hubinter G, et al. *In vitro* evaluation of bendamustine induced apoptosis in B-chronic lymphocytic leukemia. Leukemia. 2002; 2096-2105.

16. Fong PC, Boss DS, Yap TA, et al. Inhibition of poly(ADP-ribose) polymerase in tumors from BRCA mutation carriers. N Engl J Med. 2009; 361: 123-134.

17. Puaux AL, Ong, LC, Jin Y, et al. A comparison of imaging techniques to monitor tumor growth and cancer progression in living animals. Int J Mol Imaging. 2011; 2011: 1-12.

18. Radhakrishnan SK, Bebb DG, Lees-Miller SP. Targeting ataxia-telangiectasia mutated deficient malignancies with Poly ADP ribose polymerase inhibitors. Transl Cancer Res. 2013; 2: 155-162.

19. Williamson CT, Kubota E, Hamill JD, Klimowicz A, Ye R,Muzik H, et al. Enhanced cytotoxicity of PARP inhibition in mantle cell lymphoma harboring mutations in both ATM and p53. EMBO Mol Med. 2012; 4: 515-527.

20. Mahe E, Akhter A, Le A, Street L, Pournaziri P, Kosari F, et al. PARP1 expression in mantle cell lymphoma: the utility of PARP1 immunohistochemistry and its relationship with markers of DNA damage. Hematol Oncol. 2015; 33: 159-165.

21. Robson M, Im SA, Senkus E, Senkus E, Xu B, Domchek MS, et al. Olaparib for metastatic breast cancer in patients with a germline BRCA mutation. N Engl J Med. 2017; 377: 523-533.

Ann Hematol Oncol - Volume 6 Issue 2 - 2019
ISSN : 2375-7965 | www.austinpublishinggroup.com

Citation: Kiel PJ, Overholser BR, Feng H, Sinn A, Riley AA, McCarthy PB, et al. Olaparib Induced Moderate Killing of *ATM*-Deficient Mantle Cell Lymphoma Cells *In Vitro* and *In Vivo*. Ann Hematol Oncol. 2019; 6(2): 1233.